# Design, Synthesis, and Biological Evaluation of *β*-Ketosulfonamide Adenylation Inhibitors as Potential Antitubercular Agents

Jagadeshwar Vannada,[†] Eric M. Bennett,[†] Daniel J. Wilson,[†] Helena I. Boshoff,[‡] Clifton E. Barry, III,[‡] and Courtney C. Aldrich*,[†]

Center for Drug Design, Academic Health Center, University of Minnesota, Minneapolis, Minnesota 55455, and Tuberculosis Research Section, National Institute of Allergy and Infectious Diseases, Rockville, Maryland 20852-1742

aldri015@umn.edu

ABSTRACT
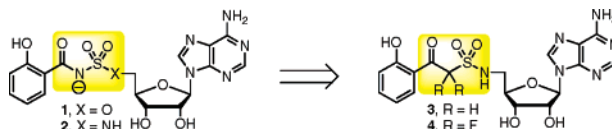
The antitubercular nucleoside antibiotics 1 and 2 were recently described that inhibit the adenylate-forming enzyme MbtA and disrupt biosynthesis of the virulence-conferring siderophore known as mycobactin in *Mycobacterium tuberculosis*. Herein, we report efforts to refine this inhibitor scaffold by replacing the labile acylsulfamate linkage (highlighted) with the more chemically robust *β*-ketosulfonamide linkage of 3 and 4.

Mycobacterium tuberculosis, the etiological agent of tuberculosis (TB), is the leading bacterial cause of infectious disease mortality.[1] The development of *M. tuberculosis* strains which are resistant to all of the current front-line antitubercular drugs has prompted worldwide efforts to discover new antibiotics to treat this notorious pathogen. Iron acquisition is an essential process for *M. tuberculosis* as well as almost all other microorganisms.[2] However, this essential micronutrient is highly sequestered in a mammalian host. Bacteria have evolved a variety of mechanisms to obtain this vital nutrient, but the most common mechanism involves the synthesis of small-molecule iron chelators, termed siderophores.[3] *M. tuberculosis* produces a pair of related peptidic siderophores known as mycobactin-T **8** and carboxymycobactins **9** that vary by the appended lipid residue and will hereafter be referred to collectively as the mycobactins (Figure 1).[4] The critical role of the mycobactins for growth and virulence of *M. tuberculosis* is supported by substantial

in vitro and in vivo evidence.[5] Therefore, inhibition of mycobactin biosynthesis[6] or antagonism of mycobactin function[7] represents an attractive strategy for the development of a new class of antitubercular agents.

The biosynthesis of the mycobactins is initiated by MbtA, an adenylate-forming enzyme, which activates salicylic acid **5** at the expense of ATP to form salicyl-adenylate **6** that remains tightly bound to the enzyme with expulsion of pyrophosphate (Figure 1).[8] MbtA then catalyzes the transfer of **6** onto a carrier domain of MbtB to provide **7**, which is ultimately extended to the mycobactins through the activity of almost a dozen additional proteins.[8,9]

Nucleoside analogues **1** and **2** were designed as stable intermediate mimetics of **6** and found to inhibit MbtA

[†] University of Minnesota.

[‡] National Institute of Allergy and Infectious Diseases.

(1) *Tuberculosis Handbook*; World Health Organization: Geneva, 1998 (WHO/TB/98.253).

(2) Ratledge, C.; Dover, L. G. *Annu. Rev. Microbiol.* **2000**, *54*, 881.

(3) Crosa, J. H.; Walsh, C. T. *Microbiol. Mol. Biol. Rev.* **2002**, *66*, 223.

(4) (a) Vergne, A. F.; Walz, A. J.; Miller, M. J. *Nat. Prod. Rep.* **2000**, *17*, 99. (b) Snow, G. A. *Bacteriol. Rev.* **1970**, *34*, 99.

(5) (a) De Voss, J. J.; Rutter, K.; Schroeder, B. G.; Su, H.; Zhu, Y.; Barry, C. E., III. *Proc. Natl. Acad. Sci. U.S.A.* **2000**, *97*, 1252. (b) Luo, M.; Fadeev, E. A.; Groves, J. T. *Nat. Chem. Biol.* **2005**, *1*, 149. (c) Wagner, D.; Maser, J.; Lai, B.; Cai, Z.; Barry, C. E., III; zu Bentrup, K. H.; Russell, D. G.; Bermudez, L. E. *J. Immunol.* **2005**, *174*, 1491.

(6) (a) Ferreras, J. A.; Ryu, J.-S.; Lello, F. D.; Tan, D. S.; Quadri, L. E. N. *Nat. Chem. Biol.* **2005**, *1*, 29. (b) Somu, R. V.; Boshoff, H.; Qiao, C.; Bennett, E. M.; Barry, C. E., III; Aldrich, C. C. *J. Med. Chem.* **2006**, *49*, 31. (c) Miethke, M.; Bisseret, P.; Beckering, C. L.; Vignard, D.; Eustache, J.; Marahiel, M. A. *FEBS J.* **2006**, *273*, 409.
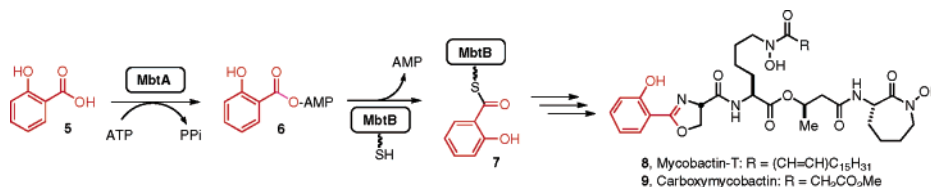
Figure 1. Biosynthesis of the mycobactins.

potently.[6] These compounds also disrupted mycobactin biosynthesis and inhibited growth of *M. tuberculosis* H37Rv under iron-limiting conditions.[6a,b] We recognized that hydrolysis of the acylsulfamate and acylsulfamide linkages of **1** and **2** would release 5′-*O*-(sulfamoyl)adenosine **10** or its amino congener **11**, which are among the most potent cytotoxic compounds yet reported (Figure 2).[10] The potential for
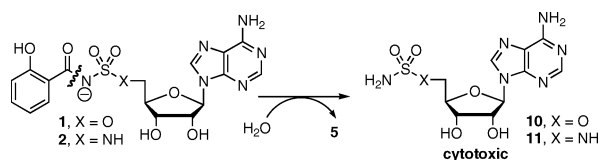

Figure 2. Hydrolysis to cytotoxic sulfamoyladenosines.

such a reaction through in vivo metabolism could lead to severe toxicity of these antibacterial agents. Furthermore, both **1** and **2** are ionized at physiological pH, which may limit oral bioavailability.[6b] To simultaneously address these potential shortcomings, we replaced the central nitrogen atom of the acylsulfamide linker of **2** with a carbon atom, which was expected to prevent undesirable hydrolysis as well as to increase the lipophilicity. The change of the sulfamide moiety to a sulfonamide function was further motivated by the prevalance of the sulfonamide group in numerous therapeutic agents including antiinfectives, antidiabetics, and diuretics.[11]

Herein, we report the synthesis of *β*-ketosulfonamide analogues **3** and **4** featuring a novel Claisen-like condensation to assemble the *β*-ketosulfonamide followed by Mitsunobu coupling to attach the adenosyl subunit. The in vitro enzyme inhibition of **3** and **4** and in vivo activity against whole cell *M. tuberculosis* have been evaluated. Further, molecular modeling provided important insight into the binding of these adenylation inhibitors to MbtA.

Several methods to synthesize *β*-ketosulfonamides have been reported including reaction of enamines with *N*-alkylsulfamoyl chlorides,[12a] treatment of silyl enol ethers with *N*-methylsulfamoyl imines,[12b] coupling of primary amines with *N*-aroylmethylsulfonyl derivatives,[12c] and condensation of *N*-alkyl sulfonamides with a nitrile.[12d] We sought an efficient synthesis of the *β*-ketosulfonamide targets that would enable the facile introduction of the nucleoside subunit and allow the rapid synthesis of the *β*-ketosulfonamide moiety; however, none of the aforementioned methods were

suitable for these demands. Our retrosynthetic analysis involves disconnection of **3** by Mitsunobu reaction to *N*-Boc-*β*-ketosulfonamide **12** (Figure 3).[13] Further retrosynthesis leads to *N*-Boc-methylsulfonamide **13**.
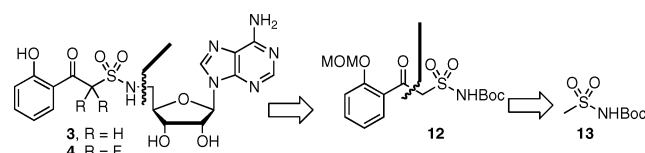
Figure 3. Retrosynthetic analysis.

Synthesis commenced with addition of LDA to **13**[14] to afford dianion **14** (Scheme 1).[15] Next, a solution of MOM-

Scheme 1. Synthesis of *β*-Ketosulfonamide
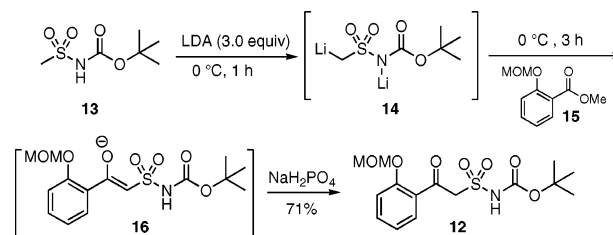
protected salicylate derivative **15** was added to provide *β*-ketosulfonamide **12**. The third equivalent of LDA was necessary to enolize the resultant *β*-ketosulfonamide to **16** preventing overaddition. This simple reaction represents a new entry into the *β*-ketosulfonamide function.

We next turned our attention to the key Mitsunobu reaction to couple a suitably protected adenosine derivative with

(7) Xu, Y.; Miller, M. J. *J. Org. Chem.* **1998**, *63*, 4314.

(8) Quadri, L. E. N.; Sello, J.; Keating, T. A.; Weinreb, P. H.; Walsh, C. T. *Chem. Biol.* **1998**, *5*, 631.

(9) Krithika, R.; Marathe, U.; Saxena, P.; Ansari, M. Z.; Mohanty, D.; Gokhale, R. S. *Proc. Natl. Acad. Sci. U.S.A.* **2006**, *103*, 2069.

(10) Bloch, A.; Coutsogeorgopoulos, C. *Biochemistry* **1971**, *10*, 4394.

(11) Lednicer, D.; Mitscher, L. A. *The Organic Chemistry of Drug Synthesis*; Wiley: New York, 1998; Vol. 6.

(12) (a) Bender, A.; Günther, D.; Willms, L.; Wingen, R. *Synthesis* **1985**, 66. (b) Vega, J. A.; Molina, A.; Alajarín, R.; Vaquero, J. J.; García-Navio, J. L.; Alvarez-Builla, J. *Tetrahedron Lett.* **1992**, *33*, 3677. (c) Hendrickson, J. B.; Bergeron, R. *Tetrahedron Lett.* **1970**, *5*, 345. (d) Thompson, M. E. *Synth. Commun.* **1988**, 733.

β-ketosulfonamide **12**.[13] Initial attempts to couple **12** and 2,3-isopropylidene adenosine **17** were unsuccessful (not shown). We speculated that this failure might be due to the competitive cyclization between N-3 and C-5' of the activated species as we observed consumption of the alcohol with formation of an extremely polar product.[16] Installation of a Boc-carbamate at N^6 of the adenine served to attenuate the nucleophilicity of N-3 and suppress this undesired reaction. Successful Mitsunobu coupling to afford **19** was achieved by addition of DIAD via syringe pump to a stirring solution of the β-ketosulfonamide **12**, N^6-Boc-adenosine **18**, and TPP at 0 °C (Scheme 2). Optimization of these conditions revealed

Scheme 2. Mitsunobu Coupling
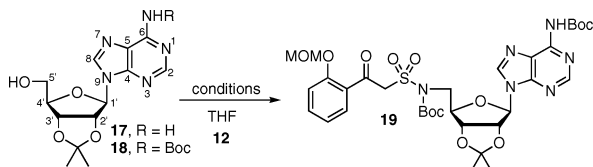
that the DIAD addition time was the most crucial parameter, thus the yield improved from 23% to 82% by increasing the addition time of DIAD from 5 to 30 min (Table 1, entries

Table 1. Optimization of Mitsunobu Reaction Conditions

| entry	phosphine (equiv)	azodicarboxylate (equiv)	addition time of DIAD (min)	time (h)	yield **19** (%)
1	TPP (2.0)	DIAD (2.0)	5	12	23
2	TPP (1.5)	DIAD (1.5)	10	12	46
3	TPP (1.5)	DIAD (1.3)	30	12	82
4	TPP (1.5)	DIAD (1.3)	30	48	0
5	F-TPP (1.5)	F-DIAD (1.3)	30	12	85

1−3). Attempts to further improve the yield by increasing the total reaction time were unsuccessful (Table 1, entry 4), which we speculate is due to the condensation with dicarboalkoxyhydrazine (DCH) to afford an enamine adduct (not shown).[17] Thus, the optimal reactions identified herein involve the slow addition of DIAD over 30 min to a cooled (0 °C) solution of the substrates and TPP followed by stirring for 12 h at 23 °C.

Although these optimized conditions worked well, isolation of **19** was challenging requiring multiple chromatographic separations. Indeed, the application of the Mitsunobu reaction is often limited by the difficulty involved in isolating

(13) Henry, J. R.; Marcin, L. R.; McIntosh, M. C.; Scola, P. M.; Harris, G. D., Jr.; Weinreb, S. M. *Tetrahedron Lett.* **1989**, *30*, 5709.

(14) Neustadt, B. R. *Tetrahedron Lett.* **1994**, *35*, 379.

(15) (a) Harter, W. G.; Albrecht, H.; Brady, K.; Caprathe, B.; Dunbar, J.; Gilmore, J.; Hays, S.; Kostlan, C. R.; Lunney, B.; Walker, N. *Bioorg. Med. Chem. Lett.* **2004**, *14*, 809. (b) Thompson, M. E. *J. Org. Chem.* **1984**, *49*, 1700. (c) Johnson, D. C., II; Widlanski, T. S. *J. Org. Chem.* **2003**, *68*, 5300.

(16) Mitsunobu, O. *Synthesis* **1981**, 1.

the pure product from a crude reaction mixture containing excess and spent reagents. The fluorous approach employing fluorous DIAD (named as F-DIAD) along with fluorous TPP (named as F-TPP) enables the rapid purification of Mitsunobu reactions by fluorous solid-phase extraction (FSPE).[18] Utilizing F-TPP and F-DIAD and our optimized reaction conditions, we were able to obtain **19** in 85% yield by simple filtration of the crude reaction mixture through a fluorous SiO_2 cartridge (Table 1, entry 5).

The synthesis of β-ketosulfonamide **3** was completed by simultaneous deprotection of the MOM acetal, isopropylidene ketal, and Boc carbamates employing aqueous TFA (Scheme 3). Fluorination of the active methylene of **19** with Selectfluor

Scheme 3. Synthesis of Final Targets
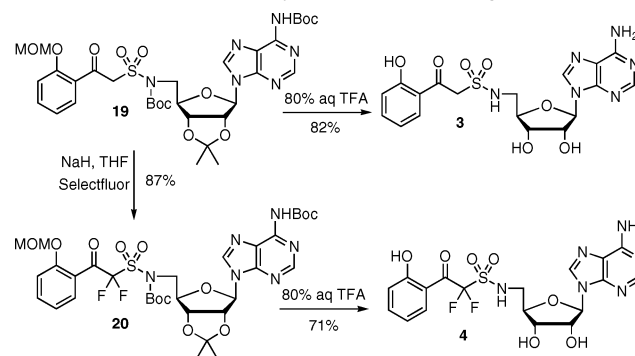
provided **20**, which was deprotected to yield α,α-difluoro-β-ketosulfonamide **4**.[19]

Next, inhibition of recombinant MbtA by the bisubstrate inhibitors was measured using a $[^{32}P]PPi−ATP$ exchange assay to determine K_I^{app} values (Table 2).[6a,20] In addition to

Table 2. MIC$_{99}$ and K_I^{app} Values of Bisubstrate Inhibitors

inhibitor	K_I^{app} (μM)	MIC$_{99}$ (μM)
1	0.00507 ± 0.00106	0.29[a]
2	0.00375 ± 0.00058	0.19[a]
3	3.30 ± 0.57	25
4	>100	>100
10	>100	50
21	>100	>100[a]

[a] See ref 6b.

3 and **4** whose synthesis is described in this paper, we also evaluated **1**, **2**, **10**, and **21** (see Figure 4B)[6b] that we had previously synthesized but not examined for enzyme inhibition.[6b] These additional analogues provided important SAR data. β-Ketosulfonamide **3** displayed modest inhibition of MbtA with a K_I^{app} of 3.30 ± 0.57 μM, and **4** showed no

(17) HRMS calcd $C_{41}H_{59}N_8O_{15}S$ [M + H]$^+$ 935.3815, found 935.3717 (error 10.5 ppm).

(18) Dandapani, S.; Curran, D. P. *J. Org. Chem.* **2004**, *69*, 8751.

(19) (a) Lal, G. S. *J. Org. Chem.* **1993**, *58*, 2791. (b) Ladame, S.; Willson, M.; Périé, J. *Eur. J. Org. Chem.* **2002**, 2640.
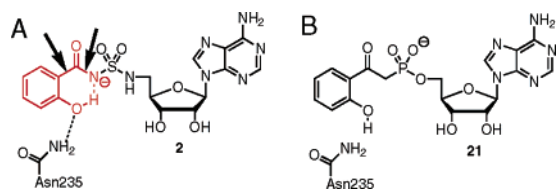
Figure 4. Proposed hydrogen-bonding arrangements. Highly active compounds (A) have linkers which readily adopt a planar geometry stabilized by an internal hydrogen bond, whereas some inactive compounds (B) have linkers which do not readily adopt a planar geometry.

inhibition at the maximum concentration evaluated ($K_I^{app} > 100$ μM). By contrast, the parent acylsulfamide inhibitor **2** exhibited potent inhibition with a K_I^{app} of 0.0038 ± 0.0006 μM. Additionally, β-ketophosphonate **21** was inactive ($K_I^{app} > 100$ μM).

To investigate the structural basis for activity, compounds **2**–**4**, the natural acyl phosphate intermediate **6**, and β-ketophosphonate **21**[6b] (Figure 4B) were docked into our homology model based on the X-ray structure of DhbE, which performs the analogous adenylation of 2,3-dihydroxybenzoic acid.[6b] Molecular mechanics simulations of the ligands free from the constraints of the protein binding site showed that some compounds did not prefer the planar linker conformation observed in the X-ray structure. Although many enzymes must release their products quickly and therefore may have reduced affinity for their products, MbtA must retain the acyl phosphate for transfer to MbtB. Therefore, the acyl phosphate's conformational preference may be relevant for inhibitor design.

To confirm the molecular mechanics results, the docked conformations were truncated at the 5′ carbon and reoptimized free from the constraints of the active site at the B3LYP/6-311G++(d,p) level. The sums of the absolute values of the deviation from planarity of the two bonds about the β-carbonyl are summarized in Table 3 (see Figure 4A: arrows denote bonds of interest). The natural acyl phosphate **6** and the highly potent inhibitor **2** adopted a nearly planar geometry similar to that observed for the acyl phosphate in the X-ray structure.[21] In contrast, **3**, **4**, and **21** deviated

Table 3. Total Torsional Deviation from Planarity around the Inhibitor β-Keto Group

compound	deviation from planarity (docked[a] in protein)	deviation from planarity (QM-optimized)[b]
2	31°	1°
3	18°	67°
4	17°	52°
6[c]	29°	14°
21	19°	140°

[a] Docked to an MbtA homology model using MacroModel. [b] Optimized in the absence of binding site constraints using Jaguar. [c] In the X-ray structure of DhbE, the bound phosphate product deviates from planarity by 7°.

significantly from planarity, with energy differences of 6.6 kcal/mol or larger relative to the docked conformation.

Interestingly, these results held only when the compounds were modeled with the aryl hydroxyl donating a hydrogen bond to the α atom (in the case of the acylsulfamate and acylsulfamide linkers, the α-nitrogen is expected to be deprotonated[6b]). When the hydroxyl hydrogen was instead oriented in the opposite direction to donate a hydrogen bond to the side chain of Asn235, all compounds became less planar during the QM optimization (data not shown; residues are numbered as in DhbE).

Because **4** and **21** were inactive while the K_I^{app} of **3** was reduced approximately 1000-fold relative to **2**, we hypothesize that linker planarity, stabilized by an internal hydrogen bond (Figure 4A), may be important for inhibition of MbtA. In this case, the Asn235 side chain must present its amino group to the inhibitor, a conformation which is consistent with the 150-fold loss of activity observed when the aryl hydroxyl is replaced with an amino group (data not shown).[5a]

The minimum concentrations of **3**, **4**, and **10** that inhibited >99% of growth of *M. tuberculosis* H37Rv under iron-deficient conditions[5a] were determined and are shown in Table 2. Compound **3** exhibited an MIC$_{99}$ of 25 μM, and **4** was inactive. The correlation of K_I^{app} and MIC$_{99}$ values of **1**–**4** under iron-deficient conditions provides support for the designed mechanism of action. Additionally, 5′-*O*-(sulfamoyl)adenosine **10** displayed an MIC$_{99}$ of 50 μM, thus the potent activity of **1** and **2** is not due to hydrolysis of these to release **10** or **11**, respectively.

In summary, we have developed an efficient synthesis of β-ketosulfonamide adenylation inhibitors featuring a newly developed Claisen-type condensation and the fluorous version of the Mitsunobu reaction to install the nucleoside subunit of the bisubstrate inhibitors. In this study, we have extended our investigation of the structure–activity relationships of the nucleoside bisubstrate inhibitors. The compromise in potency of **3** is offset by its anticipated improved ADMET profile. Modification of the nucleoside subunit of the inhibitor scaffold to regain potency and further improve upon desirable pharmacological properties is the focus of current efforts.

Supporting Information Available: Experimental procedures, compound characterization data and ^{1}H and ^{13}C NMR of compounds reported herein, details of the [^{32}P]PPi–ATP exchange assay to determine K_I^{app} values, molecular modeling, and growth inhibition assay of *M. tuberculosis* H37Rv under iron-deficient conditions. This material is available free of charge via the Internet at http://pubs.acs.org.

OL0617289

(20) Linne, U.; Marahiel, M. A. *Methods Enzymol.* **2004**, *388*, 293.
(21) May, J. J.; Kessler, N.; Marahiel, M. A.; Stubbs, M. T. *Proc. Natl. Acad. Sci. U.S.A.* **2002**, *99*, 12120.